Published in final edited form as:
Arch Biochem Biophys. 2008 March 15; 471(2): 126–133. doi:10.1016/j.abb.2008.01.003.

Dose Dependent Effects of Reactive Oxygen and Nitrogen Species on the Function of Neuronal Nitric Oxide Synthase

Jian Sun, **Lawrence J. Druhan**, and **Jay L. Zweier***
Davis Heart and Lung Research Institute, Division of Cardiovascular Medicine, Department of Internal Medicine, College of Medicine, Ohio State University, Columbus, OH 43210

Abstract

Reactive nitrogen species (RNS) and oxygen species (ROS) have been reported to modulate the function of nitric oxide synthase (NOS); however, the precise dosedependent effects of specific RNS and ROS on NOS function are unknown. Questions remain unanswered regarding whether pathophysiological levels of RNS and ROS alter NOS function, and if this alteration is reversible. We measured the effects of peroxynitrite ($ONOO^-$), superoxide ($O_2^{\cdot -}$), hydroxyl radical (·OH), and H_2O_2 on nNOS activity. The results showed that NO production was inhibited in a dose-dependent manner by all four oxidants, but only $O_2^{\cdot -}$ and $ONOO^-$ were inhibitory at pathophysiological concentrations (≤ 50 μM). Subsequent addition of tetrahydrobiopterin (BH_4) fully restored activity after $O_2^{\cdot -}$ exposure, while BH_4 partially rescued the activity decrease induced by the other three oxidants. Furthermore, treatment with either $ONOO^-$ or $O_2^{\cdot -}$ stimulated nNOS uncoupling with decreased NO and enhanced $O_2^{\cdot -}$ generation. Thus, nNOS is reversibly uncoupled by $O_2^{\cdot -}$ (≤ 50 μM), but irreversibly uncoupled and inactivated by $ONOO^-$. Additionally, we observed that the mechanism by which oxidative stress alters nNOS activity involves not only BH_4 oxidation, but also nNOS monomerization as well as possible degradation of the heme.

Keywords

neuronal nitric oxide synthase; nitric oxide; superoxide; peroxynitrite; hydroxyl; hydrogen peroxide; dose-dependent; uncoupling; tetrahydrobiopterin; monomerization

Introduction

Nitric oxide (NO) is a critical mediator of a number of biological processes including vasodilation, neurotransmission and host-defense [1-3]. Its roles in the cardiovascular system include regulation of vasomotor tone, cell adhesion to the endothelium, inhibition of platelet aggregation, and vascular smooth muscle cell proliferation [4-7]. NO is synthesized

Corresponding Author: Jay L. Zweier, Davis Heart & Lung Research Institute, The Ohio State University, 473 W 12th Avenue, Columbus, OH 43210, USA, Office, 614-247-7857 Phone, 614-247-7845 Fax, jay.zweier@osumc.edu.

in cells by a class of L-arginine dependent nitric oxide synthases (NOS) that catalyze the transformation of L–arginine to L–citrulline with the formation of NO [8-10]. There are three major isoforms of NOS. Neuronal (nNOS) and endothelial (eNOS) isoforms are constitutively expressed and require micromolar concentrations of free Ca^{2+} for activitation, via a calmodulin dependent mechanism, whereas the inducible isozyme (iNOS) is cytokine-inducible and largely Ca^{2+} independent.

The NOS enzymes are dimeric in their active form and are associated with two molecules of calmodulin (CaM). They contain relatively tightly-bound cofactors such as BH_4, FAD, FMN and iron protoporphyrin IX (heme) [11]. The catalytic domains of NOS include a flavin containing NADPH-binding reductase, and a heme-binding oxygenase that also contains the binding sites for BH_4 and L-arginine. These two domains are separated by a CaM binding sequence and in the presence of calcium/calmodulin, and the substrate NADPH, electrons flow from the reductase domain to the oxygenase domain resulting in the activation of oxygen at the heme center, followed by monooxygenation of substrate. The production of NO from L-arginine by NOS occurs via two sequential monooxygenation events, consuming 1.5 equivalents of NADPH for every NO produced [12]. Our laboratory and several others have demonstrated that besides synthesizing NO, all three isoforms of NOS can also generate $O_2^{\cdot -}$, depending on substrate and cofactor availability [13-18]. With low levels or total absence of L– arginine, purified nNOS catalyzes the reduction of oxygen, with $O_2^{\cdot -}$ production [13,14]. In L-arginine-depleted cells, nNOS generates both $O_2^{\cdot -}$ and NO leading to peroxynitrite-mediated cell injury [15].

Besides the availability of enzyme substrates or cofactors [19-21], several additional mechanisms also can modulate NO synthesis by NOS. These include protein-protein interactions [22-26], protein phosphorylation [27-29], endogenous inhibitory N-methylated L-arginines [30,31], subcellular localization [32], subunit dimerization [33], as well as product feedback inhibition, by which excess NO down-regulates the amount of subsequent NO synthesis. NOS activity can also be altered by oxidative stress.

Oxidative stress often occurs at low levels under normal physiological conditions and is greatly enhanced in a variety of disease processes associated with inflammation or ischemia and reperfusion. There are several biologically important reactive oxygen species (ROS), including $O_2^{\cdot -}$, $\cdot OH$ and H_2O_2. $O_2^{\cdot -}$ combines with NO to produce $ONOO^-$, a cytotoxic oxidant. $ONOO^-$ and ROS are chemically unstable and highly reactive, and may induce oxidative damage to DNA, lipids, and proteins. While it has been hypothesized that cellular oxidants interact with NOS and alter its activity, questions remain regarding the precise dose-dependent effects of these oxidants on the activity of the enzyme and the mechanisms involved in this process.

To characterize the specific dose dependent effects of specific reactive oxygen or nitrogen species on the enzymatic function of nNOS, purified enzyme was pre-exposed to known amounts of $O_2^{\cdot -}$, $\cdot OH$, H_2O_2 and $ONOO^-$, and the NO generation rate was quantified spectroscopically by measuring the rapid oxidation of oxyhemoglobin to methemoglobin. The NO and $O_2^{\cdot -}$ generation was also measured using electron paramagnetic resonance spin

trapping. The mechanism by which oxidative stress alters nNOS enzyme function was also explored.

Materials and methods

Materials

Human embryonic kidney (HEK) 293 cells stably transfected with rat nNOS were provided by Dr. Valina Dawson, Department of Neuroscience, The John Hopkins University, School of Medicine. Cell culture materials were obtained from GIBCO (Invitrogen, Carlsbad, CA). Peroxynitrite was purchased from Upstate Cell Signaling Solutions (Lake Placid, NY). BH_4 was obtained from Cayman Chemical Company (Ann Arbor, MI). Calmodulin and catalase were purchased from Sigma-Aldrich (St. Louis, MO). 2′ 5′ ADP Sepharose™ 4B, calmodulin Sepharose™ 4B and Superdex 200 10/300 GL Tricorn™ high performance chromatography columns and gel filtration calibration kits were purchased from Amersham Pharmacia Biosciences (Pittsburgh, PA). 5-(Diisopropoxyphosphoryl)-5-methyl-1-pyrroline-N-oxide (DIPPMPO) was from Alexis Biochemicals, Inc. (San Diego, CA). N-methyl-D-glucamine dithiocarbomate (MGD) was synthesized in our laboratory. Xanthine oxidase (XO) and complete EDTA-free protease inhibitor cocktail tablets were purchased from Roche Applied Sciences (Indianapolis, IN). All other chemicals were obtained from Sigma-Aldrich unless noted otherwise.

nNOS enzyme purification

The nNOS-transfected HEK 293 cells were cultured in DMEM supplemented with 10% heat-inactivated fetal bovine serum and antibiotics penicillin G (100 unit/ml) and streptomycin (100 μg/ml) with L-glutamine (292 μg/ml) at 37°C in a 5% CO_2, 95% air-humidified incubator. NOS expressing cells were selected for by including Geneticin® (500 μg/ml) in the growth medium. To scale up the number of cells cultured, nNOS-HEK293 cells were grown in suspension in two 1000 ml-spinner bottles for 4 days. Cells were then harvested by centrifugation and homogenized in buffer that contained 50 mM Tris-HCl, pH 7.4, 2 mM EDTA, 2 mM EGTA, 1 mM dithiothreitol (DTT) and protease inhibitors. The cell lysate was centrifugated at 16,000 g for 10 min at 4°C and the supernatant loaded onto a 2′, 5′-ADP-Sepharose 4B column. After extensive washing with 50 mM Tris-HCl, pH 7.4 with 450 mM NaCl, the bound protein was eluted with 10 mM NADPH in 50 mM Tris-HCl, pH 7.4. The eluate was then applied to a calmodulin Sepharose 4B column and equilibrated in 50 mM Tris-HCl, 150 mM NaCl, and 2 mM $CaCl_2$, pH 7.4. nNOS was eluted with 5 mM EGTA in 50 mM Tris-HCl, 150 mM NaCl, pH 7.4. The peak nNOS containing fractions were concentrated using an Amicon Ultra 100,000 MW cut off concentrator. The nNOS enzyme was stored in liquid nitrogen in 50 mM Tris-HCl pH 7.4 with 10% glycerol. The nNOS concentration was determined using the Bradford assay (Bio-Rad) with bovine serum albumin as the standard. The purity of nNOS was verified by SDS-PAGE followed by Coomassie Blue staining. The typical activity of nNOS was between 150 and 200 nmol mg^{-1} min^{-1} with a purity > 85% as determined by SDS-PAGE.

Peroxynitrite and ROS treatment of nNOS

Purified nNOS at 0.5 μg/μl (~ 1.56 μM dimer) was preincubated with BH_4 25 μM and NADPH 25 μM on ice for 30 min to allow BH_4 and NADPH to bind to nNOS. The BH_4 and NADPH saturated nNOS was exposed to given amounts of each of four oxidants: $ONOO^-$, $O_2^{\cdot -}$, OH and H_2O_2. For $ONOO^-$, exposure of nNOS to 0.2 μM to 2000 μM concentrations of $ONOO^-$ was performed on ice for 10 min. $ONOO^-$ concentration was determined by absorbance at 302 nm (ε_{302} = 1.67 $mM^{-1}cm^{-1}$). The $ONOO^-$ stock, in 0.3 M NaOH, ~ 150 mM, was diluted in 10 mM NaOH to various concentrations just before addition to the nNOS solution in 50 mM Tris-HCl pH 7.4. The volume of $ONOO^-$ added was limited to 1/10 of the total incubation volume. Since the half-life of peroxynitrite in neutral solution is less than 2 sec, there was no need for a quenching step for the $ONOO^-$ treatment. For $O_2^{\cdot -}$ exposure, the generating system consisted of 0.1 unit/ml XO, with xanthine in a concentration range from 0.2 μM to 2000 μM, and 200 unit/ml catalase to remove any H_2O_2 formed. $O_2^{\cdot -}$ produced from xanthine-XO was quantitated using the cytochrome c reduction assay and the concentration of $O_2^{\cdot -}$ generated corresponded to ~ 50% of the xanthine concentration. BH_4 and NADPH saturated nNOS samples were incubated for 20 min at room temperature with this xanthine-XO system and then SOD (1000 unit/ml) as well as additional catalase 200 unit/ml were added to quench any residual $O_2^{\cdot -}$ production from xanthine-XO and the preparation placed on ice. For OH exposure, OH was generated from H_2O_2 via the iron mediated Fenton reaction as reported previously [34]. Ferric iron chelate Fe^{3+} - nitrilotriacetate (Fe-NTA) (1:2) was prepared according to the literature [35]. The BH_4 and NADPH saturated nNOS was incubated with 20 μM Fe-NTA and H_2O_2 (0.2 μM to 2000 μM H_2O_2) on ice for 20 min and any excess H_2O_2 was removed by the addition of 400 unit/ml catalase. For H_2O_2 exposure, the BH_4 and NADPH saturated nNOS samples were incubated with given amounts of H_2O_2 in the presence of 400 μM diethylenetriaminepentaacetic acid (DTPA). After 20 min incubation on ice, catalase 400 unit/ml was added. For all exposures 5 min were allowed between completion of exposure and measurement of nNOS activity.

Oxyhemoglobin assay of NO generation rate

nNOS activity was measured from the initial rate of NO generation spectrophotometrically determined from the oxidation of oxyhemoglobin to methemoglobin. The NO generation rate was calculated from the change in the absorption at 401 nm minus 411 nm as a function of time ($\varepsilon_{401\text{-}411}$ = 38 mM^{-1} cm^{-1}) [36]. The assay mixture consisted of the control or oxidant exposed nNOS in 50 mM Tris-HCl, pH 7.4, as described above, with 200 μM $CaCl_2$, 10 μg/ml CaM, 150 μM DTT, 200 μM NADPH and 10 μM oxyhemoglobin added. 100 μM L-arginine was added to start the reaction. To test the effect of BH_4 repletion, matched experiments were performed with addition of 100 μM BH_4. These assays were carried out on a plate-reader, SPECTRA Max Plus 384 from Molecular Devices, with 96-well plates at 37°C. The NO generation rate was determined using the data collected in the linear phase of the change in absorbance at 401 – 411 nm within the first two minutes.

EPR spin trapping of $O_2^{\cdot -}$ and NO

Spin trapping measurements of NO and $O_2^{\cdot -}$ generation form nNOS were performed using a Bruker EMX EPR spectrometer with HS cavity in a 50μl capillary tube. The NO assay mixture contained 40 μg/ml purified nNOS, 0.2 mM Fe-MGD (1:10) spin trap (ammonium iron (II) sulfate 0.2mM, MGD 2 mM) and nNOS substrates and co-factors (200 μM $CaCl_2$, 10 μg/ml CaM, 1 mM NADPH, 2 mM ^{15}N-L-arg) in 50 mM Tris-HCl, pH 7.4, The $O_2^{\cdot -}$ assay mixture consisted of 40 μg/ml nNOS, 500 unit/ml catalase, 400 μM DTPA, nNOS substrates and co-factors (as above) and 20 mM DIPPMPO spin trap. For the determination of the effects of $ONOO^-$ and $O_2^{\cdot -}$ nNOS was incubated with either 50 μM $ONOO^-$ on ice or with 100 μM Xanthine and XO 0.1 unit/ml at room temperature for 10 min. In the later case 500 μM oxypurinol was added to assure terminatation of any XO-mediated $O_2^{\cdot -}$ generation 1 min before starting the spin trap measurements. All EPR spectra were obtained in a 50 μl capillary tube at room temperature (23°C) using the following parameters: microwave power 20 mW, modulation frequency 100 kHz, microwave frequency 9.87 GHz, time constant of 163.84 mSec, and scan time 84 s. The modulation amplitude used for NO and $O_2^{\cdot -}$ detection was 4.0 G and 1.0 G, respectively. All EPR spectra shown are accumulation of 5 scans.

Gel filtration Chromatography for detection of nNOS dimer and monomer

The nNOS samples were subjected to gel filtration chromatography on Superdex 200 HR column controlled by an AKTA™design fast protein liquid chromatography (FPLC) system (Amersham Pharmacia Biotech). The column was equilibrated with 50 mM Tris-HCl, pH 7.4 with 150 mM NaCl at 4°C. The nNOS was eluted at a flow rate of 0.3 ml/min and monitored by UV/Visible absorbance at 280 nm, 254 nm and 400 nm. The calibration curve was obtained based on the elution profiles of protein standards (thyroglobulin, ferritin, catalase, aldolase, albumin, and ovalbumin). The void volume was determined with Dextran Blue 2000. The areas of the peaks of dimer and monomer were integrated using the chromatography software package, Unicorn 4.0 (Amersham).

Statistical Analysis

Results were expressed as mean ± SE. Statistical significance was determined using the Student's t - Test. A value of $P < 0.05$ was considered statistically significant.

Results

Effects of oxidative stress on NO generation rate by nNOS

The rate of NO generation from nNOS was significantly decreased following exposure to increasing levels of $ONOO^-$ (Fig. 1). The rate of NO production following exposure to 20 μM $ONOO^-$ decreased to 66% of basal levels and with 100 μM $ONOO^-$ decreased to 42% of basal activity with progressively increasing inhibition at higher concentrations. With all $ONOO^-$ concentrations studied, subsequent addition of BH_4 only very modestly restored enzyme function with a maximum BH_4-dependent restoration of +14 % in NO generation seen following 500 μM $ONOO^-$ exposure. With the highest concentration studied, 2000 μM $ONOO^-$, addition of BH_4 did not restore any nNOS activity.

Similar to $ONOO^-$, $O_2^{\cdot-}$ dose dependently decreased the NO generation rate by nNOS (Fig. 2). With exposure to 20 μM xanthine, corresponding to 10 μM total measured $O_2^{\cdot-}$ generation, NO production decreased to 81% of baseline and with 100 μM Xanthine (50 μM $O_2^{\cdot-}$ generation) to 44%. However, BH_4 addition was able to almost completely rescue the loss of nNOS activity induced by these low levels of $O_2^{\cdot-}$ exposure. Even with 100 μM xanthine, subsequent addition of BH_4 restored the activity to almost 95% of basal levels. At higher xanthine concentrations, only partial nNOS activity was recovered with BH_4 addition. Thus BH_4 addition was highly effective in reversing the $O_2^{\cdot-}$-induced loss of nNOS activity at low to moderate levels of $O_2^{\cdot-}$generation, while higher levels as seen with 1000 or 2000 μM xanthine no significant restoration of NO generation was seen.

Exposure to OH generated from the H_2O_2/Fe-NTA generating system resulted in loss of NO production only at high levels of H_2O_2, with 65% of basal activity remaining at 500 μM H_2O_2 and 52% activity with 1000 μM H_2O_2 (Fig. 3). However, unlike $O_2^{\cdot-}$, there was no significant BH_4-induced rescue of enzyme activity lost during OH treatment. In stark contrast to the other three oxidants, H_2O_2 had very little effect on nNOS activity until very high concentrations were used (Fig. 4). H_2O_2 treatment had no significant effect on NO generation rate at concentrations less than 2000 μM (Fig. 4). With 2000 μM H_2O_2 exposure, 61 % activity was still present and addition of BH_4 did not significantly restore this loss of nNOS activity.

Effects of oxidative stress in inducing nNOS uncoupling with $O_2^{\cdot-}$ generation

To determine and definitively demonstrate that oxidative stress induces nNOS uncoupling, leading to $O_2^{\cdot-}$ generation, EPR spin trapping measurements were performed. Purified nNOS (0.5 μg/μl, ∼3.12 μM) was incubated under anaerobic conditions in the presence of 4 μM BH_4 and NADPH on ice for 30 min at to allow BH_4 and NADPH binding to nNOS. This BH_4 and NADPH saturated nNOS was then incubated either with 50 μM $ONOO^-$ on ice or with the $O_2^{\cdot-}$ generating system using 100 μM xanthine - 0.1 unit/ml XO at RT for 10 min. EPR measurements were carried out as described in the experimental section with the nitrone spin trap DIPPMPO, which forms a relatively stable $O_2^{\cdot-}$ adduct. The effects of $ONOO^-$ and $O_2^{\cdot-}$ exposure on subsequent $O_2^{\cdot-}$ generation, were then determined in the presence of 2 mM ^{15}N-L-arg by adding nNOS co-factors (200 μM $CaCl_2$, 20 μg/ml CaM, 1 mM NADPH). Control nNOS gave only a very weak EPR signal, in contrast, $ONOO^-$ and $O_2^{\cdot-}$ treated nNOS gave rise to a strong DIPPMPO-OOH signal characteristic of trapped $O_2^{\cdot-}$ (Fig.5 left panel).

Parallel experiments were carried out to determine the effects of $ONOO^-$ and $O_2^{\cdot-}$ on NO release from nNOS using the well characterized NO spin trap Fe-MGD. A strong NO signal from nNOS was observed exhibiting the characteristic doublet spectrum of the ^{15}NO·Fe·MGD complex. ^{15}N isotopically labeled L-arginine was used to prove that the nitrogen was derived from the guanidino group of L-arginine and also to ensure that only NO from nNOS was measured. In the presence of L-arginine, both $ONOO^-$ (50 μM) and $O_2^{\cdot-}$ (50 μM) significantly inhibited NO formation observed from nNOS (Fig.5 right panel). Thus, from these studies both $ONOO^-$ (50 μM) and $O_2^{\cdot-}$ (50 μM), decrease NO production and greatly enhance $O_2^{\cdot-}$ generation. As such, at this level of oxidant exposure, as occurs

under a range of pathophysiological conditions, both $ONOO^-$ and $O_2^{\cdot -}$ induce uncoupling of nNOS and greatly enhance nNOS-derived $O_2^{\cdot -}$ generation.

Effects of Oxidants on the nNOS monomer/dimer equilibrium

To explore the possible mechanisms by which oxidative stress alters nNOS enzyme function, further experiments were performed using FPLC to separate the nNOS monomer and dimer states. Purified nNOS (15 μg) with 5 mM DTT in 100 μl volume was injected to a Superdex 200 10/300 mm size exclusion column with 50 mM Tris-HCl, 150 mM NaCl, pH 7.4 as elution buffer. As seen in figure 6, the untreated nNOS is almost totally present as dimer with a retention volume of 10.1 ml. To obtain nNOS monomer, nNOS was incubated with 5 M urea on ice for 2 hours [37]. This urea treated nNOS gave 92% monomer and 8% dimer according to the peak integration of the absorbance at 280 nm. The retention volume for the monomer was 11.6 ml (Fig. 6). A significant increase in monomer peak appeared with $O_2^{\cdot -}$-treated (500 μM xanthine/0.1 XO unit/ml, 250 μM total superoxide) and $ONOO^-$ (500 μM)-treated nNOS, with levels of 50% and 33% respectively (Fig. 6, 7). OH treatment (500 μM H_2O_2) also induced less but notable monomer formation, of 21%, as seen from the shoulder peak in figure 6. However, there was no evidence of monomer formation in the 500 uM H_2O_2-treated nNOS.

In addition to the monomer/dimer analysis, the FPLC studies provided data on the effects of oxidants in inducing changes in the optical absorbance of nNOS dimer and monomer. For the $O_2^{\cdot -}$, $ONOO^-$, OH and H_2O_2-treated nNOS samples, absorbance at 400 nm was decreased to 75%, 61%, 89% and 96% of the untreated nNOS respectively. In contrast to this the absorbance at 280 nm showed little change with oxidant treatment. Since the absorbance at 400 nm in nNOS is due mainly to the Soret band of the heme group, the observed oxidant-induced decrease in A_{400nm} is likely related to heme degradation or a change in the heme binding site with greatest effect seen with $ONOO^-$ and lesser effects with $O_2^{\cdot -} > \cdot OH > H_2O_2$.

Discussion

Nitric oxide and oxygen radical generation is increased in postischemic tissues such as the heart and brain and mediate postischemic injury [38,39]. It is well known that oxygen radicals cause lipid peroxidation and cellular calcium loading both of which are critical processes of cellular injury [34,40]. Reactive oxygen and nitrogen species formed in postischemic tissues may alter NOS function and all three NOS isoforms can become potent sources of ROS with the depletion of L-arginine or BH_4 [15,18]. While it is known that oxidants can induce NOS dysfunction, there has been a lack of knowledge regarding the precise dose-dependent relationships by which particular biological oxidants alter NOS function and which oxidants exert the greatest concentration dependent effects. Furthermore, it is unknown if levels of ROS or $ONOO^-$formed under pathophysiological conditions lead to a loss of NOS function or induce uncoupling of the enzyme.

nNOS was the first of the NOS isoforms shown to generate $O_2^{\cdot -}$ and it is present at high levels in brain and other neurons as well as other tissues [13,14,41]. In the absence of L-arginine or with BH_4 depletion, production of NO from nNOS becomes uncoupled from the

oxidation of NADPH, resulting in prominent $O_2^{\cdot-}$ generation [12]. Loss of NO production from NOS would exert profound effects on neuronal function and signaling. Uncoupling of the enzyme with $O_2^{\cdot-}$ formation would also further shift the balance of NO and $O_2^{\cdot-}$ present and likely induce cellular injury. However, the precise sensitivity of this critical enzyme to specific oxidant stress has not been determined.

Under pathophysiolgical conditions of oxidant stress as occur in ischemic and reperfused tissues, it can be inferred that the total integrated fluxes of ROS formation of $O_2^{\cdot-}$, OH, or H_2O_2 result in total concentrations from several μM to 100 μM values [42-44]. Similar values would also be expected for $ONOO^-$ [38]. In the current study, we observed that both $ONOO^-$ and $O_2^{\cdot-}$ significantly alter nNOS function at levels above 10 - 20 μM while at levels above 100 μM >50% reduction in nNOS activity was seen. In contrast to this, for H_2O_2-derived OH relatively high > 200 uM exposures were required to induce significant alterations in nNOS activity. Moreover, treatment with H_2O_2 had very little effect even at very high concentrations, treatment with >1 mM H_2O_2 were required to produce even only modest effects. This resistance to oxidation by H_2O_2 is consistent with previous data demonstrating that nNOS can use H_2O_2 as a substrate, with formation of the reactive heme-oxy species, followed by reaction with N^{ω}-hydroxyl-L-arginine or L-arginine [45,46].

With NOS that was pre-exposed to $ONOO^-$, subsequent addition of BH_4 produced only a modest restoration of NO generation. Similarly, for OH or H_2O_2-treated nNOS, subsequent addition of BH_4 did not restore nNOS activity. This demonstrates that the oxidation of BH_4 is not the only cause of the loss of NO generation by nNOS for these oxidants. In contrast, subsequent addition of BH_4 to $O_2^{\cdot-}$-treated nNOS completely restored the NO generation at low and moderate levels of $O_2^{\cdot-}$-exposure (≤50 μM), and still significantly restored NO generation even after treatment with much higher levels of $O_2^{\cdot-}$. Thus, the $O_2^{\cdot-}$-induced decrease in NO activity is almost completely due to BH_4 oxidation until very high concentrations are reached.

Oxidant induced decreases in enzyme activity have been noted previously in many enzyme systems, including the NOS isozymes, and a number of different mechanisms have been implicated. Laursen *et al.* [47] and others [48,49] have reported that $ONOO^-$ is more potent than either $O_2^{\cdot-}$ or H_2O_2 in causing oxidation of BH_4. These investigators reported that $ONOO^-$ dramatically increased vascular $O_2^{\cdot-}$ production in vessels from control mice but not in vessels from eNOS-deficient mice, suggesting that eNOS was the source of $O_2^{\cdot-}$ [48]. Our results agree that $ONOO^-$ is a potent inhibitor of nNOS-directed NO generation, however, our data indicates that BH_4 oxidation is only one component of the oxidant-induced nNOS dysfunction. Furthermore, with the exception $O_2^{\cdot-}$, BH_4 oxidation does not appear to be the most significant cause of the oxidant-induced decrease in NO generation by nNOS.

It has been well demonstrated that under certain conditions NOS enzymes can produce $O_2^{\cdot-}$, either in lieu of or in addition to NO, and that the oxidation state of the BH_4 plays a critical role in coupling electron transfer from NADPH to L-arg to prevent the production of $O_2^{\cdot-}$ [20]. NOS catalysis functions via two sequential monooxygenation events which require the generation of a stable activated oxygen species at the heme center. In the absence of BH_4, the activated oxygen species decays after a one electron reduction of molecular oxygen,

producing $O_2^{\cdot -}$ rather than NO, leading to a condition known as NOS uncoupling [18]. BH_4 not only increases NO generation by nNOS, but also decreases $O_2^{\cdot -}$ and subsequent H_2O_2 formation. When BH_4 is added to a viable "uncoupled" NOS, the oxidation of NADPH is again coupled to the production of NO, as such any oxidant-induced decrease in NO activity that can be rescued by the addition of BH_4 can be viewed as an indication of the presence of uncoupled NOS. Indeed we observed that $O_2^{\cdot -}$ exposure induced this BH_4 dependent uncoupling with reversible loss of nNOS activity. EPR spin trapping measurements also confirmed that this low level of $O_2^{\cdot -}$ exposure triggered $O_2^{\cdot -}$ generation from the enzyme. Interestingly, while $ONOO^-$ also induced a loss of activity this was much less reversible with subsequent BH_4 addition. Low level $ONOO^-$ exposure also triggered $O_2^{\cdot -}$ generation. This data together with the demonstrated inability of BH_4 to rescue ONOO− induced enzyme dysfunction indicates that peroxynitrite-dependent uncoupling occurs by an additional mechanism independent of BH_4.

For eNOS, it has been reported that an increase of eNOS-dependent $O_2^{\cdot -}$ formation correlated with the decrease in eNOS dimer levels in endothelial cells BAECs treated with $ONOO^-$ [49]. Our EPR results with purified nNOS demonstrate that $ONOO^-$ and $O_2^{\cdot -}$ induced a increase in $O_2^{\cdot -}$ generation in the presence of BH_4 and L-arg, which is consistant with results reported in cultured cells [50,51] where $ONOO^-$ and oxidative stress switch nNOS from NO generation to $O_2^{\cdot -}$ generation. To begin to define the molecular mechanisms responsible for the observed oxidant-induced decrease in enzyme activity, we determined the change in nNOS monomer:dimer ratio after oxidant treatment. It is know that treatment with urea can dissociate the dimer into stable monomers [52]. Our FPLC results showed that a significant amount of nNOS monomer was generated by treatment with either $O_2^{\cdot -}$ or $ONOO^-$, while ·OH treatment produced a lesser amount of monomer. However, there was almost no detectible dissociation of the dimer in H_2O_2–treated nNOS. As expected, oxidant induced nNOS monomerization mirrors the observed activity decrease, that is, the more potent the oxidant in decreasing nNOS activity the higher amount of monomerization occured. Electron transfer from the reductase domain to the oxygenase domain is a requisite inter-subunit transfer [23]. Therefore, monomerization of nNOS is a key mechanism contributing to the oxidant-induced loss of nNOS activity.

Questions remain regarding how oxidant stress induces nNOS monomerization. Low temperature SDS-PAGE and gel filtration studies have demonstrated that BH_4 stabilizes the nNOS dimer against dissociation [37,52,53]. This could partially explain the observed monomerization of $ONOO^-$ and ROS-treated nNOS. BH_4 is oxidized when nNOS is exposed to $ONOO^-$ and ROS, and the stability of nNOS dimer would be decreased due to the depletion of BH_4. It is known that reconstitution of pterin-free iNOS with BH_4 can recover function to that of the active enzyme [54]. However, our results show that oxidant treatment sufficient to induce loss of nNOS activity, with the exception of low levels of $O_2^{\cdot -}$ exposure, leads to an irreversible decrease in NO production and immediate addition of BH_4 did not significantly restore the loss of nNOS activity. Therefore, oxidation of BH_4 leading to the subsequent decrease in dimer stability is not the only mechanism involved in the oxidant-induced decrease of nNOS activity.

Analysis of the gel filtration data gives some evidence that the heme or the heme binding site is a target for oxidation. Integration of the peaks elucidated that there is an absorbance decrease at 400 nm. The observed changes in the absorbance of 400 nm could be indicative of oxidation of the heme and possibly decreased heme content of the enzyme after exposure to $O_2^{\cdot -}$, $ONOO^-$, $\cdot OH$ and H_2O_2. $ONOO^-$ induced the highest decrease in A_{400}, which correlates well with the irreversible dose-dependent loss of nNOS activity. Previous studies have shown that the heme group of nNOS is required for enzyme dimerization and that heme-free NOS is monomeric [55]. As such, oxidation of the heme moiety that leads to degradation would not only inactivate the enzyme, but would also lead to the observed monomerization. Another interesting point of the gel filtration data is that although $O_2^{\cdot -}$ induces the most nNOS monomer, the hypothesized heme loss is in the order of $ONOO^- > O_2^{\cdot -} > \cdot OH > H_2O_2$. This could explain why subsequent addition of BH_4 can restore the observed loss in NO generation induced by $O_2^{\cdot -}$, but is not able to rescue the $ONOO^-$ induced decrease. Exogenous $O_2^{\cdot -}$ mainly induces BH_4 oxidation at low or moderate concentrations, while $ONOO^-$ primarily induces irreversible damage, potentially to the heme group.

Conclusion

Our studies show that NO production from purified nNOS was decreased in a dose-dependent manner by the oxidants $ONOO^-$, $O_2^{\cdot -}$, $\cdot OH$ and H_2O_2. Pathophysiological levels of $ONOO^-$ and $O_2^{\cdot -}$, were sufficient to cause prominent loss of NO generation from nNOS and result in uncoupling of the enzyme. $\cdot OH$ and H_2O_2 only altered nNOS at high levels. $ONOO^-$ and $O_2^{\cdot -}$ – induced oxidative stress leading to uncoupling of nNOS even in the presence of L-arg with an increase in nNOS-derived $O_2^{\cdot -}$ generation. The decrease in NO generation of nNOS induced by $ONOO^-$, $\cdot OH$ and H_2O_2 was not significantly restored with the subsequent addition of BH_4, however, with $O_2^{\cdot -}$ exposure at low and moderate levels near total restoration of function was seen. Our results indicate that oxidant-induced enzyme dysfunction occurs via both oxidation of BH_4 and other mechanisms including potential degradation or loss of the heme center, with subsequent monomerization of the active homodimer

Acknowledgments

This work was supported by the National Institutes of Health Grants HL63744, HL65608, and HL38324, to J.L.Z.

References

1. Ignarro LJ. Annu Rev Pharmacol Toxicol. 1990; 30:535–560. [PubMed: 2188578]
2. Bredt DS, Snyder SH. Neuron. 1992; 8:3–11. [PubMed: 1370373]
3. Marletta MA, Tayeh MA, Hevel JM. Biofactors. 1990; 2:219–225. [PubMed: 2282138]
4. Palmer RMJ, Ferrige AG, Moncada S. Nature. 1987; 327:524–526. [PubMed: 3495737]
5. Kubes P, Suzuki M, Granger DN. Proc Natl Acad Sci U S A. 1991; 88:4651–4655. [PubMed: 1675786]
6. Radomski MW, Palmer RMJ, Moncada S. Trends Pharmacol Sci. 1991; 12:87–88. [PubMed: 1647064]
7. Scottburden T, Vanhoutte PM. Circulation. 1993; 87:51–55.
8. Marletta MA. Cell. 1994; 78:927–930. [PubMed: 7522970]

9. Nathan C, Xie QW. Cell. 1994; 78:915–918. [PubMed: 7522969]
10. Knowles RG, Moncada S. Biochem J. 1994; 298:249–258. [PubMed: 7510950]
11. Ghosh DK, Stuehr DJ. Biochemistry. 1995; 34:801–807. [PubMed: 7530045]
12. Stuehr DJ, Kwon NS, Nathan CF, Griffith OW, Feldman PL, Wiseman J. J Biol Chem. 1991; 266:6259–6263. [PubMed: 1706713]
13. Pou S, Pou WS, Bredt DS, Snyder SH, Rosen GM. J Biol Chem. 1992; 267:24173–24176. [PubMed: 1280257]
14. Heinzel B, John M, Klatt P, Bohme E, Mayer B. Biochem J. 1992; 281:627–630. [PubMed: 1371384]
15. Xia Y, Dawson VL, Dawson TM, Snyder SH, Zweier JL. Proc Natl Acad Sci U S A. 1996; 93:6770–6774. [PubMed: 8692893]
16. Xia Y, Zweier JL. Proc Natl Acad Sci U S A. 1997; 94:6954–6958. [PubMed: 9192673]
17. Xia Y, Roman LJ, Masters BSS, Zweier JL. J Biol Chem. 1998; 273:22635–22639. [PubMed: 9712892]
18. Xia Y, Tsai AL, Berka V, Zweier JL. J Biol Chem. 1998; 273:25804–25808. [PubMed: 9748253]
19. Tayeh MA, Marletta MA. J Biol Chem. 1989; 264:19654–19658. [PubMed: 2584186]
20. Bogle RG, Baydoun AR, Pearson JD, Moncada S, Mann GE. Biochem J. 1992; 284:15–18. [PubMed: 1599394]
21. Arnal JF, Munzel T, Venema RC, James NL, Bai CL, Mitch WE, Harrison DG. J Clin Invest. 1995; 95:2565–2572. [PubMed: 7539455]
22. Bredt DS, Snyder SH. Proc Natl Acad Sci U S A. 1990; 87:682–685. [PubMed: 1689048]
23. Abusoud HM, Yoho LL, Stuehr DJ. J Biol Chem. 1994; 269:32047–32050. [PubMed: 7528206]
24. Garcia-Cardena G, Fan R, Shah V, Sorrentino R, Cirino G, Papapetropoulos A, Sessa WC. Nature. 1998; 392:821–824. [PubMed: 9580552]
25. Song Y, Zweier JL, Xia Y. Am J Physiol Cell Physiol. 2001; 281:C1819–C1824. [PubMed: 11698240]
26. Song Y, Zweier JL, Xia Y. Biochem J. 2001; 355:357–360. [PubMed: 11284722]
27. Corson MA, James NL, Latta SE, Nerem RM, Berk BC, Harrison DG. Circ Res. 1996; 79:984–991. [PubMed: 8888690]
28. Dimmeler S, Fleming I, Fisslthaler B, Hermann C, Busse R, Zeiher AM. Nature. 1999; 399:601–605. [PubMed: 10376603]
29. Nakane M, Mitchell J, Forstermann U, Murad F. Biochem Biophys Res Commun. 1991; 180:1396–1402. [PubMed: 1719982]
30. Cardounel AJ, Zweier JL. J Biol Chem. 2002; 277:33995–34002. [PubMed: 12091378]
31. Cardounel AJ, Xia Y, Zweier JL. J Biol Chem. 2005; 280:7540–7549. [PubMed: 15574418]
32. Michel T, Li GK, Busconi L. Proc Natl Acad Sci U S A. 1993; 90:6252–6256. [PubMed: 7687064]
33. Schmidt H, Pollock JS, Nakane M, Gorsky LD, Forstermann U, Murad F. Proc Natl Acad Sci U S A. 1991; 88:365–369. [PubMed: 1703296]
34. Josephson RA, Silverman HS, Lakatta EG, Stern MD, Zweier JL. J Biol Chem. 1991; 266:2354–2361. [PubMed: 1846625]
35. Aisen P, Leibman A, Zweier J. J Biol Chem. 1978; 253:1930–1937. [PubMed: 204636]
36. Kelm M, Feelisch M, Spahr R, Piper HM, Noack E, Schrader J. Biochem Biophys Res Commun. 1988; 154:236–244. [PubMed: 3260776]
37. RodriguezCrespo I, Gerber NC, deMontellano PRO. J Biol Chem. 1996; 271:11462–11467. [PubMed: 8626704]
38. Wang PH, Zweier JL. J Biol Chem. 1996; 271:29223–29230. [PubMed: 8910581]
39. Zweier JL, Fertmann J, Wei G. Antioxid Redox Signal. 2001; 3:11–22. [PubMed: 11294189]
40. Venardos KM, Kaye DM. Curr Med Chem. 2007; 14:1539–1549. [PubMed: 17584062]
41. Lafoncazal M, Pietri S, Culcasi M, Bockaert J. Nature. 1993; 364:535–537. [PubMed: 7687749]
42. Zweier JL. J Biol Chem. 1988; 263:1353–1357. [PubMed: 2826476]

43. Zweier JL, Kuppusamy P, Williams R, Rayburn BK, Smith D, Weisfeldt ML, Flaherty JT. J Biol Chem. 1989; 264:18890–18895. [PubMed: 2553726]
44. Xia Y, Zweier JL. J Biol Chem. 1995; 270:18797–18803. [PubMed: 7642530]
45. Pufahl RA, Wishnok JS, Marletta MA. Biochemistry. 1995; 34:1930–1941. [PubMed: 7531495]
46. Adak S, Wang Q, Stuehr DJ. J Biol Chem. 2000; 275:33554–33561. [PubMed: 10945985]
47. Laursen JB, Somers M, Kurz S, McCann L, Warnholtz A, Freeman BA, Tarpey M, Fukai T, Harrison DG. Circulation. 2001; 103:1282–1288. [PubMed: 11238274]
48. Landmesser U, Dikalov S, Price SR, McCann L, Fukai T, Holland SM, Mitch WE, Harrison DG. J Clin Invest. 2003; 111:1201–1209. [PubMed: 12697739]
49. Kuzkaya N, Weissmann N, Harrison DG, Dikalov S. J Biol Chem. 2003; 278:22546–22554. [PubMed: 12692136]
50. Shang TS, Kotamrajua S, Zhao HT, Kalivendi SV, Hillard CJ, Kalyanaraman B. Free Radical Biol Med. 2005; 39:1059–1074. [PubMed: 16198233]
51. Zou MH, Shi CM, Cohen RA. J Clin Invest. 2002; 109:817–826. [PubMed: 11901190]
52. Panda K, Rosenfeld RJ, Ghosh S, Meade AL, Getzoff ED, Stuehr DJ. J Biol Chem. 2002; 277:31020–31030. [PubMed: 12048205]
53. Klatt P, Schmidt K, Lehner D, Glatter O, Bachinger HP, Mayer B. EMBO J. 1995; 14:3687–3695. [PubMed: 7543842]
54. Rusche KM, Marletta MA. J Biol Chem. 2001; 276:421–427. [PubMed: 11022039]
55. Klatt P, Pfeiffer S, List BM, Lehner D, Glatter O, Bachinger HP, Werner ER, Schmidt K, Mayer B. J Biol Chem. 1996; 271:7336–7342. [PubMed: 8631754]

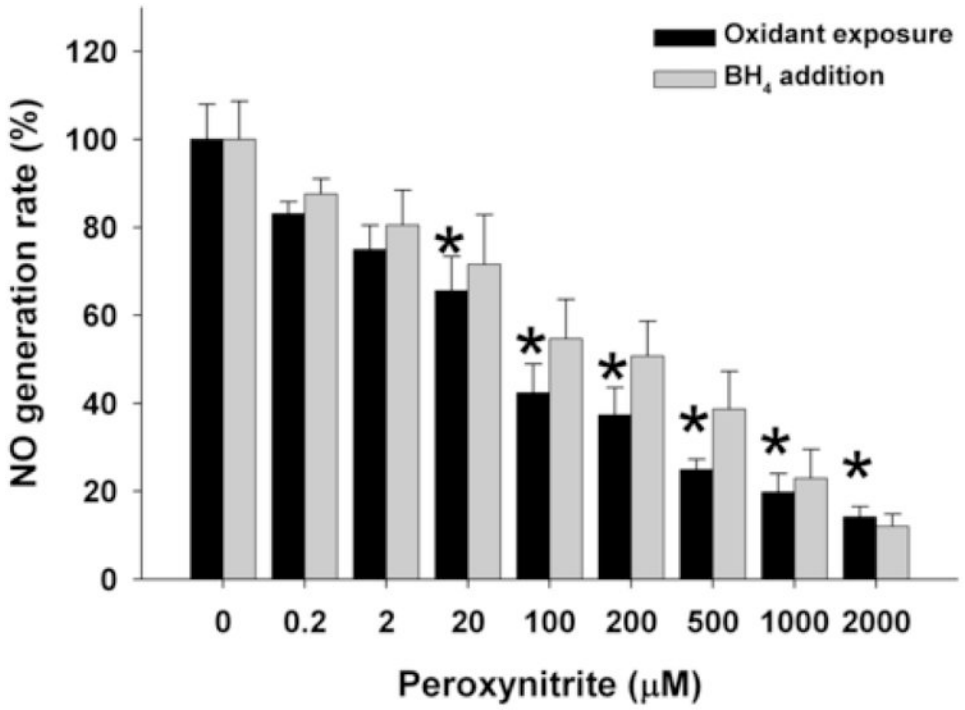

Fig. 1. Dose-dependent effect of $ONOO^-$ on NO generation rate from nNOS

BH_4 and NADPH saturated nNOS was incubated with $ONOO^-$ (0-2000 μM) for 10 min on ice. NO generation rate was then measured using the oxyhemoglobin assay in 50 mM Tris-HCl, pH 7.4 at 37°C, containing 200 μM NADPH, 200 μM $CaCl_2$, 150 μM DTT, 10 μg/ml CaM, 10 μM oxyhemoglobin, 100 μM L-Arginine, with or without subsequent addition of 100 μM BH_4. The NO generation rates were calculated from the initial rates and are given as percentage of the activity of the 0 μM $ONOO^-$-treated nNOS. Data are presented as mean ± S.E. of triplicate experiments. ***** Indicates a significant ($P < 0.05$) difference from the corresponding untreated control value.

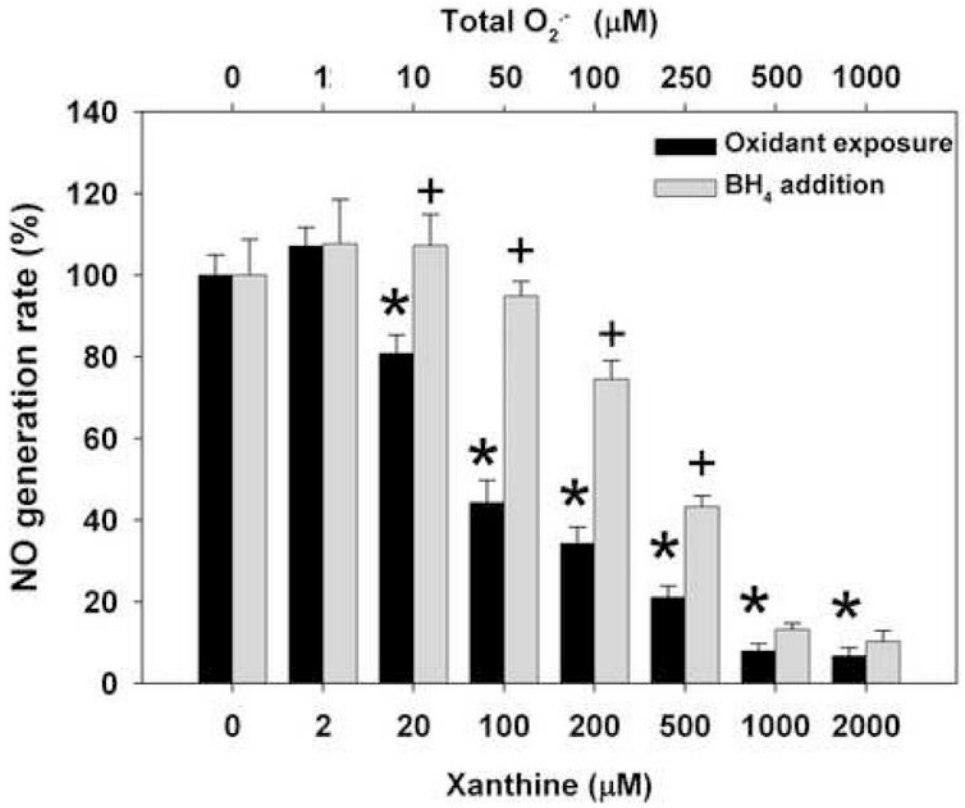

Fig. 2. Dose-dependent effect of $O_2^{\cdot-}$ on NO generation rate from nNOS

BH_4 and NADPH saturated nNOS was incubated with $O_2^{\cdot-}$ generation system, xanthine (0-2000 μM) – XO (0.1unit/ml) – catalase (200 unit/ml), for 20 min at room temperature. SOD (1000 unit/ml) and additional catalase (200 unit/ml) was then added and incubated for 5 min to terminate the reaction and remove any residual $O_2^{\cdot-}$ from xanthine-XO. NO generation rate was measured with oxyhemoglobin assay in 50 mM Tris-HCl, pH 7.4 at 37°C. The assay mixture included 200 μM NADPH, 200 μM $CaCl_2$, 150 μM DTT, 10 μg/ml CaM, 10 μM oxyhemoglobin, 100 μM L-Arginine, with or without subsequent addition 100 μM BH_4. The NO generation rates were calculated from the initial rates and are given as percentage of the activity of the 0 μM xanthine-treated nNOS. Data are presented as mean ± S.E. of triplicate experiments. ***** Indicates a significant ($P < 0.05$) difference from the corresponding untreated control value; **+** Indicates significant activity is restored by subsequent addition of BH_4 ($P < 0.05$).

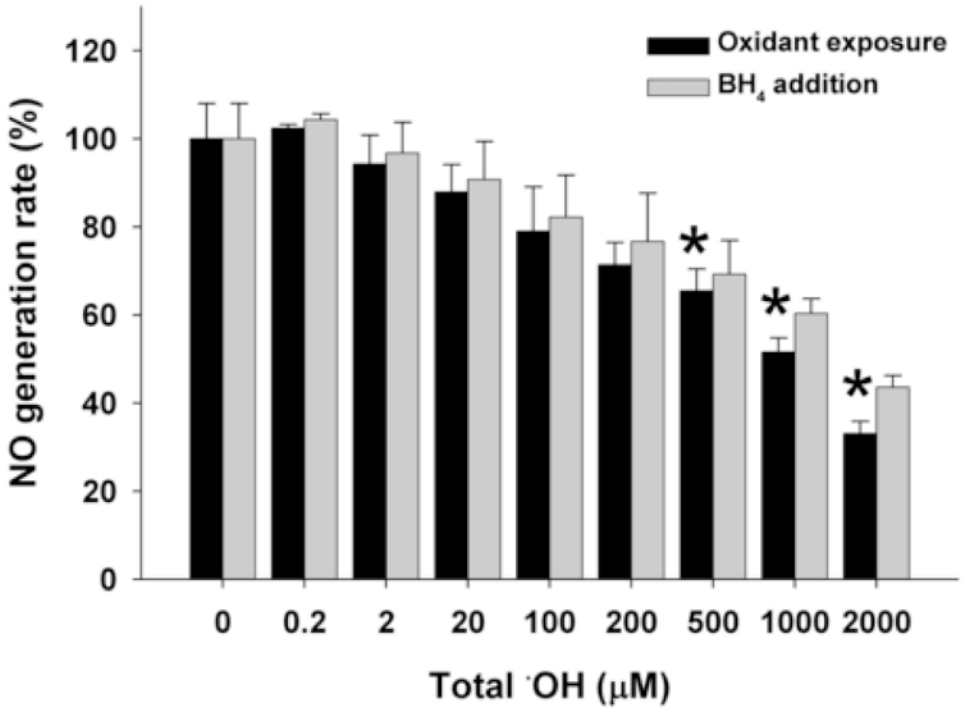

Fig. 3. Dose-dependent effect of ·OH on NO generation rate from nNOS

BH_4 and NADPH saturated nNOS was incubated with 20 μM Fe-NTA and increasing concentrations of H_2O_2 (0-2000 μM) for 20 min on ice and 400 unit/ml catalase was added to remove the residual H_2O_2 before the assay. NO generation rate was measured using oxyhemoglobin assay containing 200 μM NADPH, 200 μM $CaCl_2$, 150 μM DTT, 10 μg/ml CaM, 10 μM oxyhemoglobin, 100 μM L-Arginine, with or without subsequent addition of 100 μM BH_4. The NO generation rates were calculated from the initial rates and are given as percentage of the activity of the 0 μM OH-treated nNOS. Data are presented as mean ± S.E. of triplicate experiments. ***** Indicates a significant ($P < 0.05$) difference from the corresponding control value.

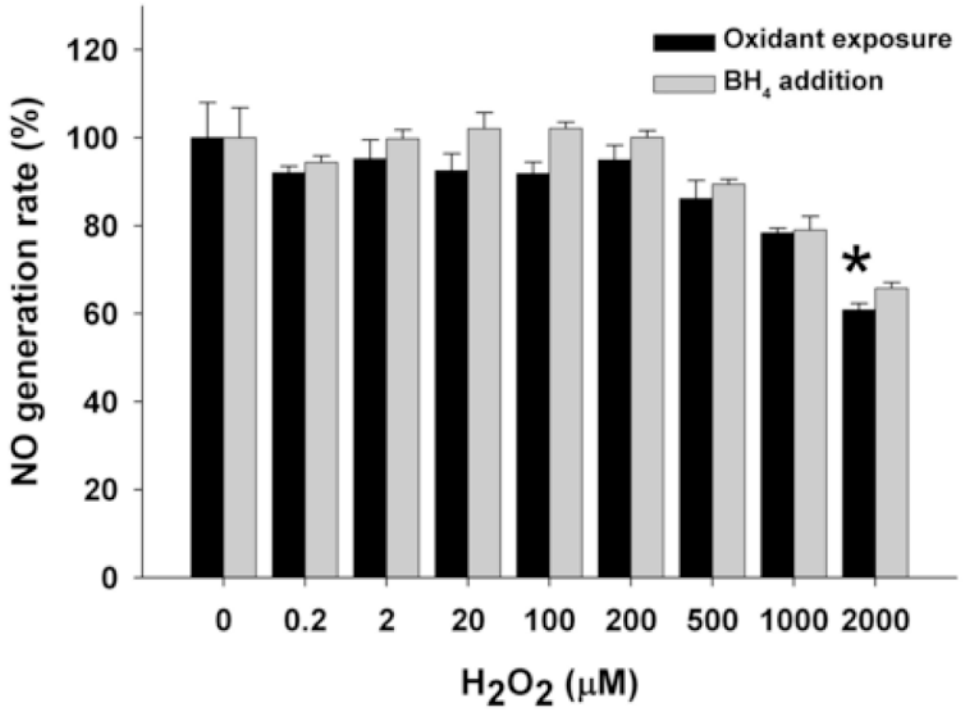

Fig. 4. Dose-dependent effect of H_2O_2 on NO generation rate from nNOS

BH_4 and NADPH saturated nNOS was incubated with 400 μM DTPA and increasing concentrations of H_2O_2 (0-2000 μM) for 20 min on ice and 400 unit/ml catalase was added to remove the residual H_2O_2 before the assay. NO generation rate was measured using oxyhemoglobin assay containing 200 μM NADPH, 200 μM $CaCl_2$, 150 μM DTT, 10 μg/ml CaM, 10 μM oxyhemoglobin, 100 μM L-Arginine, with or without subsequent addition of 100 μM BH_4. The NO generation rates were calculated from the initial rates and are given as percentage of the activity of the 0 μM H_2O_2-treated nNOS. Data are presented as mean ± S.E. of triplicate experiments. Data are presented as mean ± S.E. of triplicate experiments. ***** Indicates a significant ($P < 0.05$) difference from the corresponding untreated control.

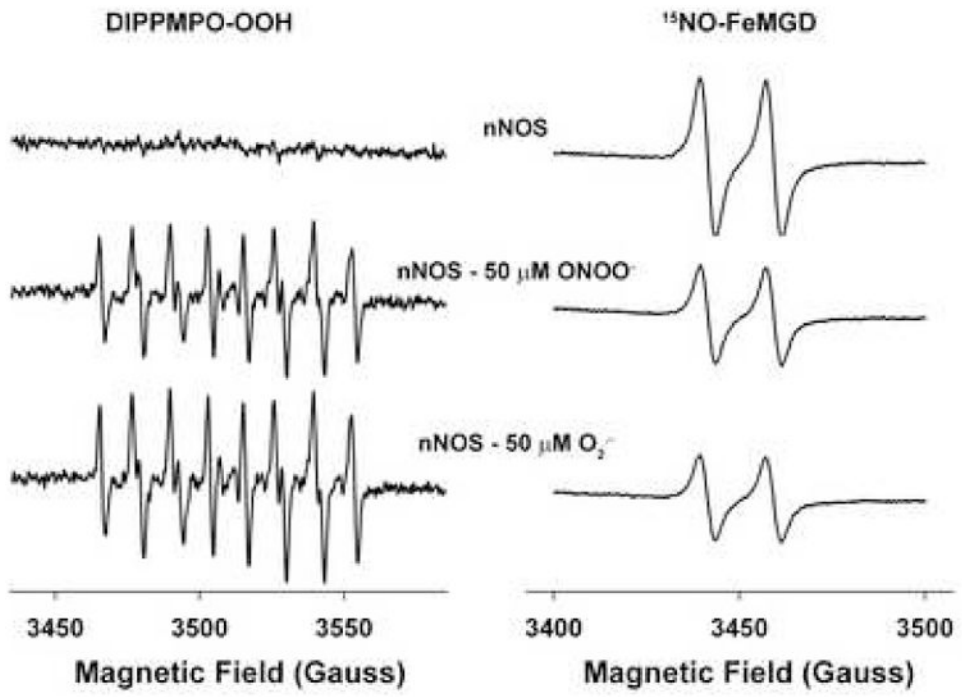

Fig. 5. Effects of $ONOO^-$ and $O_2^{\cdot -}$ on NOS-derived $O_2^{\cdot -}$ and NO generation

nNOS was exposed to 50 μM $ONOO^-$ or 50 μM $O_2^{\cdot -}$ (100 μM xanthine-0.1 uint/ml XO) on ice or at room temperature for 10 min. EPR spin trapping measurements of $O_2^{\cdot -}$ or NO production from nNOS were performed with spin trap 20 mM DIPPMPO or 0.2 mM Fe-MGD in the presence of 2 mM ^{15}N-L-arginine with 200 μM $CaCl_2$, 10 μg/ml CaM, 1 mM NADPH. EPR parameters were as described in methods. The *left panel* shows the characteristic spectra of the $O_2^{\cdot -}$-derived DIPPMPO-OOH adduct, while the *right panel* shows the NO-derived spectra of the ^{15}NO·Fe·MGD adduct.

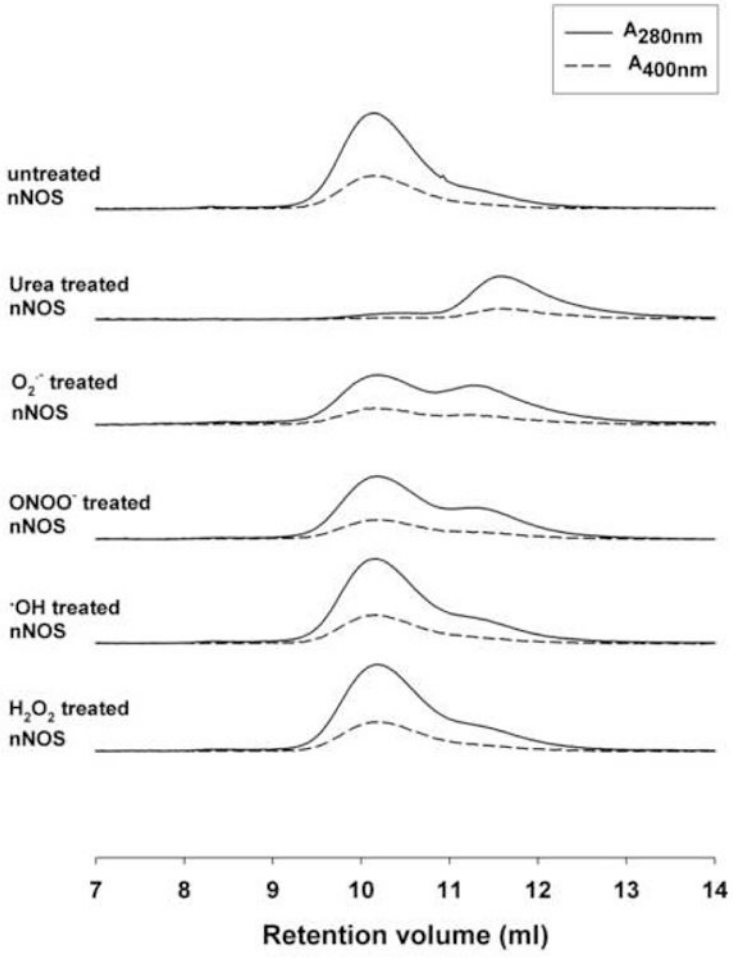

Fig. 6. FPLC profiles demonstrating effects of $ONOO^-$, ·OH and H_2O_2 on the monomerization of nNOS dimers

nNOS 15 μg was applied to each analysis. Elution buffer consisted of 50 mM Tris-HCl, 150 mM NaCl, 5 mM DTT, pH 7.4. Supedex 200 column and elution buffer were well equilibrated at ~6 °C. Above are chromatograms for untreated nNOS, 5 M urea-treated nNOS (5 M urea; 2 hours on ice), $O_2^{\cdot-}$-treated nNOS (500μM xanthine; 0.1unit/ml XO; 20 min at RT), $ONOO^-$-treated nNOS (500 μM $ONOO^-$; 10 min on ice), OH-treated nNOS (500 μM H_2O_2; 20μM Fe-NTA; 20 min on ice), and H_2O_2-treated nNOS (500 μM H_2O_2; 200μM DTPA; 20 min on ice). Solid lines present the absorbance at 280 nm wavelength. Dashed lines present the absorbance at 400 nm wavelength.

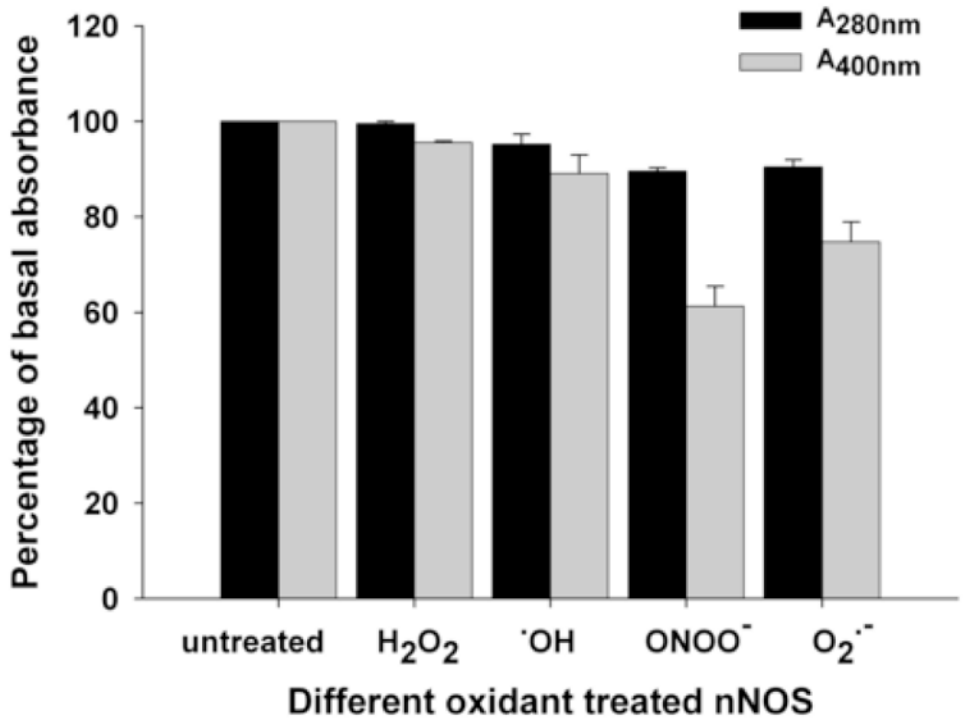

Fig. 7. Peak integration results of gel filtration chromatography

The absorbance of untreated nNOS at 280nm (black bar) and 400nm (gray bar) are used as basal control. The total absorbance of dimer and monomer peaks of oxidant treated nNOS is shown as percentage of the basal control. Data are presented as mean ± S.E. of triplicate experiments.